IOP Publishing Nanotechnology
Nanotechnology 27 (2016) 095603 (8pp) doi:10.1088/0957-4484/27/9/095603

Au/TiO_2 nanobelt heterostructures for the detection of cancer cells and anticancer drug activity by potential sensing

Jingjie Cui[1], Jing Chen[2], Shaowei Chen[3], Li Gao[4], Ping Xu[1] and Hong Li[1]

[1] College of Life Information Science & Instrument Engineering, Hangzhou Dianzi University, Hangzhou 310018, People's Republic of China
[2] Institute of Developmental and Regenerative Biology, Hangzhou Normal University, Hangzhou 310036, People's Republic of China
[3] Department of Chemistry and Biochemistry, University of California, 1156 High Street, Santa Cruz, California, 95064, USA
[4] Institute of Life Sciences, Jiangsu University, 301# Xuefu Road, Zhenjiang 212013, Jiangsu Province, People's Republic of China

E-mail: cuijingjie@hdu.edu.cn

Received 30 September 2015, revised 14 December 2015
Accepted for publication 6 January 2016
Published 29 January 2016

Abstract

Cancer is a cell dysfunction disease. The detection of cancer cells is extremely important for early diagnosis and clinical treatments. At present, the pretreatment for the detection of cancer cells is costly, complicated and time-consuming. As different species of the analytes may give rise to specific voltammetric signals at distinctly different potentials, simple potential sensing has the specificity to detect different cellular species. By taking advantage of the different electrochemical characteristics of normal cells, cancer cells and biointeractions between anticancer drugs and cancer cells, we develop a specific, sensitive, direct, cost-effective and rapid method for the detection of cancer cells by electrochemical potential sensing based on Au/TiO_2 nanobelt heterostructure electrodes that will be of significance in early cancer diagnosis, *in vitro* screening of anticancer drugs and molecular biology research.

Keywords: cancer cells, Au/TiO_2 nanobelt heterostructures, *in situ*, potential sensing, specific detection, anticancer drug screening

(Some figures may appear in colour only in the online journal)

1. Introduction

Cancer is one of the most serious and lethal diseases around the world. However, mortality is markedly reduced if it is diagnosed early. Nanotechnology has attracted great interest in the diagnosis and treatment of cancer [1]. For example, magnetoferritin nanoparticles (M-HFn) have been used to target and visualize tumour tissues [2], nanoparticles may communicate *in vivo* to amplify tumour targeting [3], carbon nanotubes are used in electronic devices for the detection of cancer cells [4, 5] and magnetic-Au nanorods are used in surface plasmon resonance biosensors for the sensitive detection of cancer [6]. As cancer is a cell dysfunction disease, cancer cells have significant differences from normal cells, including morphology, proliferation and genetic traits [7–9]. Cancer cells may release proteins into the extracellular environment, leading to overexpression of these proteins [10]. The overexpressed proteins are defined as tumour markers, which are potentially useful in screening for early malignancy [11, 12].

Notably, cancer cells exhibit markedly different cell membranes to normal cells [13]. Malignancy is associated with the altered expression of the glycans and glycoproteins that contribute to the cellular glycocalyx [14, 15]. For example, membrane proteins such as glycoproteins on the cellular surface may be overexpressed, which will greatly influence the properties of the cellular surface. Such variation may be exploited for the identification of cancer cells and

normal cells by electrochemical technology. Yet, to the best of our knowledge, there has been no report in the literature thus far.

At present, organic dyes and quantum dots are usually used for the detection of cancer cells by optical microscopic measurements. Yet the organic dyes and quantum dots are expensive and/or toxic to cells, and the pretreatment for the detection of cancer cells is complicated, time-intensive and prone to cross-contamination among samples. In contrast, electrochemical detection displays unique advantages such as fast response, high sensitivity, *in situ* monitoring, low costs and no damage to the cells. In addition, different species of analytes may give rise to specific voltammetric signals at distinctly different potentials [16]. Thus, voltammetric methods possess unique specificity in the detection of different cellular species, in contrast to techniques based on electrochemical impedance experiments where the cells are analysed by resistance changse in the system [17]. It is well known that resistance sensing has no specificity.

This is the primary motivation of the present work. Herein we report voltammetric sensing of cancer cells based on Au/TiO_2 nanobelt heterostructure electrodes. TiO_2 nanobelts are environmentally stable with unique sensing and biocompatible properties [18]. However, the high resistance of TiO_2 strongly impedes electron transfer due to its wide band gap (3.2 eV). Therefore, the development of new materials to modify TiO_2 is urgently needed to improve the electron transfer efficiency. In this study, Au/TiO_2 nanobelt heterostructures were synthesized that exhibited markedly improved electron transfer properties compared with TiO_2 nanobelts, and were employed as active materials for the detection of cancer cells and biointeractions with anticancer drugs including O6-benzylguanine (O^6BG) and 6-Thioguanine (6-TG) by potential sensing using human breast cancer cells (MDA-MB-231) and lung cancer cells as the examples. For comparison, the electrochemical behaviours of normal cells, in this case embryonic kidney cells (293 T), were also studied using the same sensing electrode. The results showed clear differences in electrochemical behaviour for the different cells that have never been reported previously. Additionally, in comparison with other electrochemical methods based on the indirect detection of cancer cells in the presence of additives such as anticancer drugs [19] or $[Fe(CN)_6]^{3-/4-}$ [20], the advantages of the present approach primarily lie in the capability for *in situ* direct detection of cancer cells, which will be of significance in early cancer diagnosis, drug screening and anticancer research.

2. Materials and methods

2.1. Materials

Titania P-25 (TiO_2, ca. 75% anatase and 25% rutile), sodium hydroxide (NaOH), hydrochloric acid (HCl) and sulfuric acid (H_2SO_4) were purchased from Sinopharm Chemical Reagents Corporation Ltd 5% Nafion (DuPont), $HAuCl_4 \cdot 4H_2O$, O^6-benzylguanine (O^6BG) and 6-Thioguanine (6-TG) were obtained from Aladdin Reagents Co., Ltd RPMI 1640 and Dulbecco's Modified Eagle Medium (DMEM, Gibco Corporation, New York), Fetal Bovine Serum (FBS, Sijiqing, China), human breast cancer cells (MDA-MB-231), embryonic kidney cells (293 T) and Lung cancer cells (A594) were obtained from the American Type Culture Collection.

2.2. Preparation of TiO_2 nanobelts and Au/TiO_2 nanobelts

Titanate nanobelts were synthesized by using a hydrothermal process in a concentrated NaOH aqueous solution. Commercial titania powders (a mixture of anatase and rutile at a ratio of 3:1) were used as the precursor. Briefly, 0.1 g of the P-25 precursor was mixed with 20 ml of a 10 M NaOH aqueous solution, followed by a hydrothermal treatment at 180 °C in a 25 ml Teflon-lined autoclave for 72 h. The treated powders were washed thoroughly with deionized water, followed by a filtration and drying process, resulting in sodium titanate nanobelts that were then immersed in a 0.1 M HCl aqueous solution for 24 h and washed thoroughly with water to produce hydrogen titanate nanobelts. These nanobelts were divided into two portions. One portion was thermally annealed at 600 °C for 2 h, leading to the formation of uncauterized TiO_2 nanobelts. The other was dispersed into 20 ml of 0.02 M H_2SO_4 aqueous solution under magnetic stirring for half an hour. The mixed solution was then transferred into a Teflon-lined stainless steel autoclave up to 80% of the total volume, heated at 100 °C for 12 h, and cooled to room temperature in air. The wet products were then thoroughly washed with deionized water and then dried at 70 °C to obtain surface-coarsened hydrogen titanate nanobelts ($H_2Ti_3O_7$). These nanobelts were then divided into two parts. The first part was thermally annealed at 600 °C for 2 h to produce surface-coarsened TiO_2 nanobelts. The other was dispersed into a $HAuCl_4 \cdot 4H_2O$ solution (at a Ti:Au mole ratio of 25:1) and then soaked for 5 h. Subsequently, the soaked samples were carefully collected from solution and dried in an oven at 110 °C overnight. Finally, the dried samples were heat-treated at 600 °C for 2 h to obtain Au/TiO_2 nanobelts.

2.3. Structure characterization

X-ray powder diffraction (XRD) patterns were obtained on a Bruker D8 Advance powder x-ray diffractometer with Cu-Ka radiation ($\lambda = 0.154\,06$ nm). X-ray photoelectron spectroscopy (XPS) measurements were performed on a Kratos Axis Ultra DLD (delay-line detector) spectrometer equipped with a monochromatic Al K_α x-ray source (1486.6 eV). All binding energies were referenced to the C1s peak at 284.8 eV of the surface adventitious carbon. High resolution transmission electron microscope (HRTEM) images were obtained with a JEOL JEM 2100 microscope. All experiments were performed at room temperature.

2.4. Electrode preparation

A glassy carbon electrode (GCE; 3 mm in diameter) was polished with 0.05 μm α-Al_2O_3 suspensions until a mirror

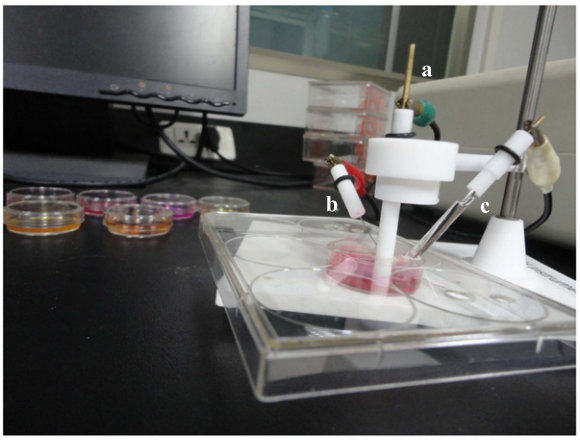

Figure 1. Three-electrode configuration for the detection of cancer cells: (a) modified nanobelt working electrode; (b) Pt wire auxiliary electrode; (c) Ag/AgCl/KCl saturated reference electrode.

surface was obtained, and rinsed extensively with anhydrous ethanol and deionized water. The electrode was then electrochemically cleaned in 0.5 M H_2SO_4 by cycling potentials between −0.3 and +1.8 V at 100 mV s^{-1} until a steady cyclic voltammogram was obtained. Nafion adhesive (2.5 μl) was drop-cast onto the cleaned GCE surface, onto which 3 μl of an ethanolic suspension of TiO_2 nanobelts or Au/TiO_2 nanobelts (0.5 mg ml^{-1}) was added in a dropwise fashion. The GCE loaded with active materials was fully dried in air, resulting in TiO_2 nanobelts or Au/TiO_2 nanobelts sensing electrodes.

2.5. In situ electrochemical investigation of cells

Normal embryonic kidney cells (293 T) and human breast cancer cells (MDA-MB-231) or human lung cancer cells (A594) were routinely cultured in 35 mm cell culture dishes at 37 °C in 5% CO_2 in DMEM/10% FBS or RPMI 1640 medium/10% FBS, 100 U ml^{-1} penicillin and 100 μg ml^{-1} streptomycin prior to use, respectively. The volume of the culture media is 2 ml in this work. Electrochemical measurements were performed in a three-electrode configuration (see figure 1) when cell density reached 80%–90% confluence. The modified nanobelt electrodes prepared as above were used as the working electrode and slowly immersed into the cell culture such that the electrode was in direct contact with cancer cells that were grown on the bottom of the culture dish, not suspended in the culture media. A Pt wire was used as the auxiliary electrode. All potentials were referred to an Ag/AgCl/KCl saturated reference electrode. Voltammetric data were acquired with a CHI 660C electrochemical workstation.

2.6. In situ electrochemical investigation of cancer cells and anticancer drug effects

Under the same experimental conditions specified above, human breast cancer cells (MDA-MB-231) or lung cancer cells (A594) were routinely cultured and the voltammetric responses were acquired before and after anticancer drugs (O6BG or 6-TG) were added in a dropwise fashion.

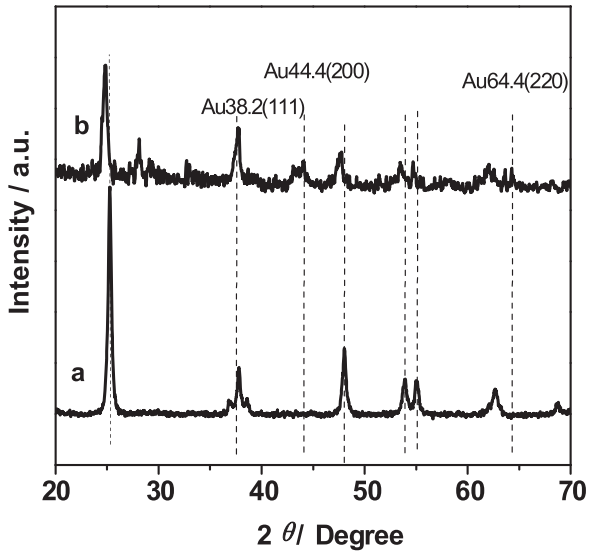

Figure 2. XRD patterns of (a) surface-coarsened TiO_2 nanobelts and (b) Au/TiO_2 nanobelts.

3. Results and discussion

3.1. Structural characterization

The structures of the TiO_2 nanobelts were first characterized by XRD measurements. In contrast to the uncauterized TiO_2 nanobelts that exhibited mixed crystalline phases (not shown), the cauterized ones showed a pure anatase phase after acid etching (figure 2(a)) [21]. For Au/TiO_2 nanobelts (figure 2(b)), in addition to the anatase features from surface-cauterized TiO_2 nanobelts, the diffraction peaks at 38.2°, 44.4°, and 64.4° can be indexed to the (111), (200) and (220) lattice planes of fcc Au [22], respectively. In addition, compared with surface-cauterized TiO_2 nanobelts (figure 2(a)), the diffraction peaks of the anatase phase exhibit a negative shift, probably because Au resulted in expansion of the TiO_2 lattice.

XPS measurements were then carried out to evaluate the elemental composition of the surface-coarsened Au/TiO_2 nanobelts. As shown in figure 3(a), the elements Ti, C, O and Au can be readily identified. Elemental carbon was likely to originate from the adhesive tape used in the XPS test. Figure 3(b)–(d) shows the high-resolution XPS spectra of the Ti2*p*, Au4*f* and O1*s* electrons, respectively. In figure 3(b), the binding energies of Ti 2*p*3/2 and 2*p*1/2 electrons were centred at 458.6 and 464.3 eV, respectively, consistent with the Ti (IV) oxidation state. The Au4*f* spectrum is composed of two peaks at 83.3 (4*f*7/2) and 87.1 (4*f*5/2) eV (figure 3(c)) [23]. In comparison to the standard binding energy of bulk Au (84.0 eV and 87.7 eV), there is a redshift of 0.6 to 0.7 eV of the Au4*f* electrons in Au/TiO_2, suggesting partial charge

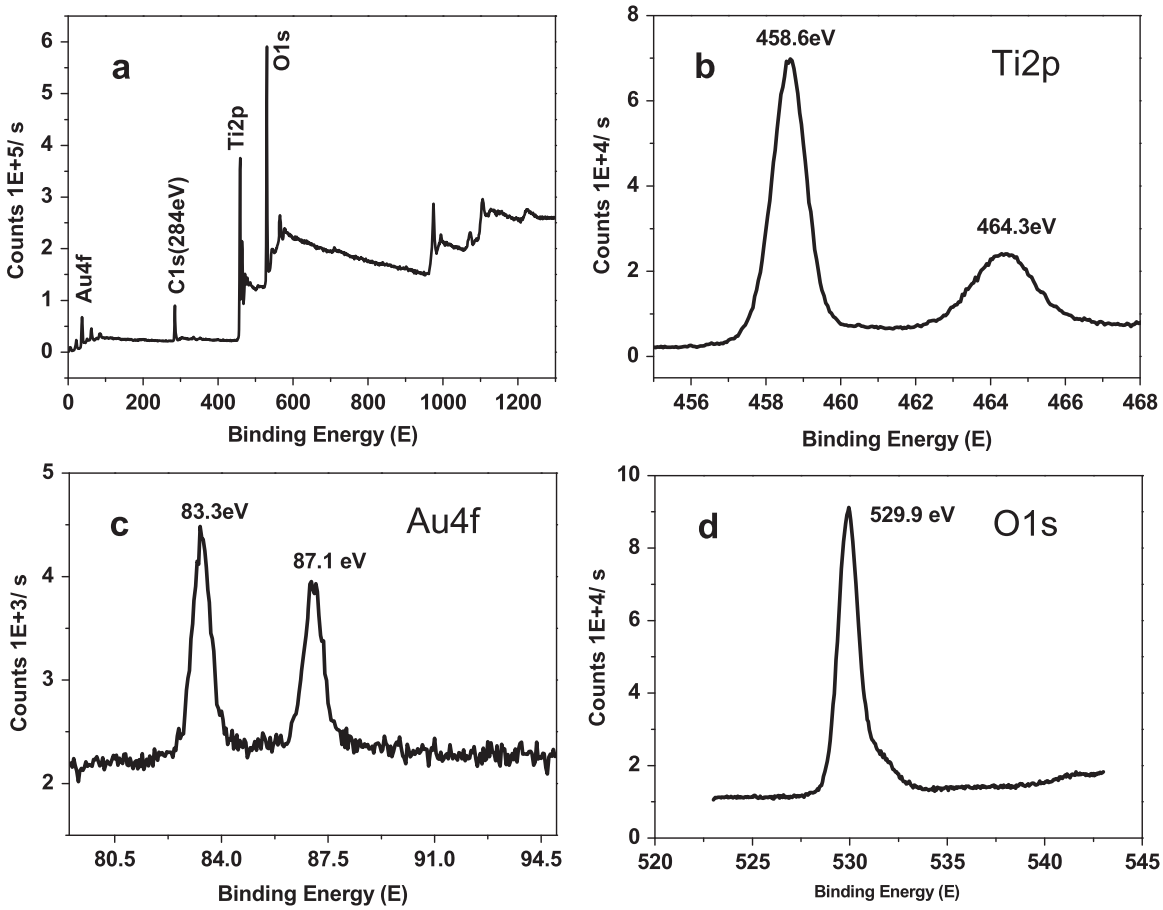

Figure 3. (a) XPS survey spectrum, and high-resolution scans of (b) Ti2p, (c) Au4f and (d) O1s electrons.

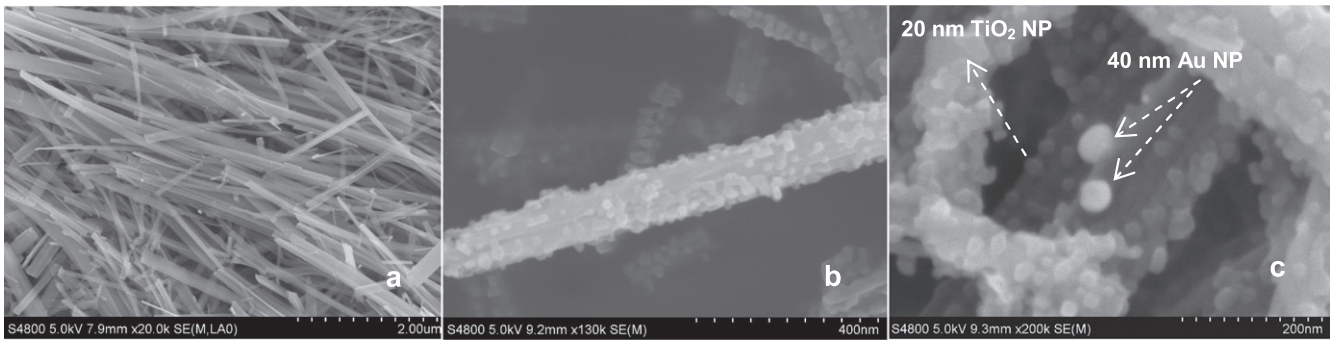

Figure 4. SEM images of (a) pre- and (b) post- coarsened TiO_2 nanobelts, and (c) Au/TiO_2 nanobelts.

transfer from titanium to gold on the TiO_2 nanobelt surface. In the high-resolution scan of the O1*s* electrons (figure 3(d)), the peak at 529.8 eV corresponds to the lattice oxygen of the TiO_2 crystal. The slight asymmetry might be ascribed to the formation of adsorbed hydroxyl species (OH·, 531.2 eV) that were generated from the interaction between trapped electrons and adsorbed water on the nanobelt surface, leading to enhanced catalytic oxidation activity of the TiO_2 nanobelts.

Figure 4 depicts representative SEM micrographs of these nanobelt samples. Panels (a) and (b) show the morphology and microstructure of the pre- and post-coarsened TiO_2 nanobelts, respectively. The pre-coarsened TiO_2 nanobelts exhibit a smooth surface (figure 4(a)), while a heterostructure was formed on the surface of the post-coarsened TiO_2 nanobelts that were coated with 20 nm TiO_2 nanoparticles (figure 4(b)). As depicted in figure 4(c), in addition to the TiO_2 nanoparticles, Au nanoparticles with a diameter of 40 nm were co-precipitated on the surface of the TiO_2 nanobelts to form a heterostructure. These TiO_2 and Au nanoparticles are anticipated to lead to a higher interfacial activity of the TiO_2 nanobelts.

In summary, an Au/TiO_2 nanobelt heterostructure with Au nanoparticles deposited onto the coarsened TiO_2 surface was successfully prepared. Structural characterizations indicate that it may exhibit enhanced catalytic activity for biosensing applications.

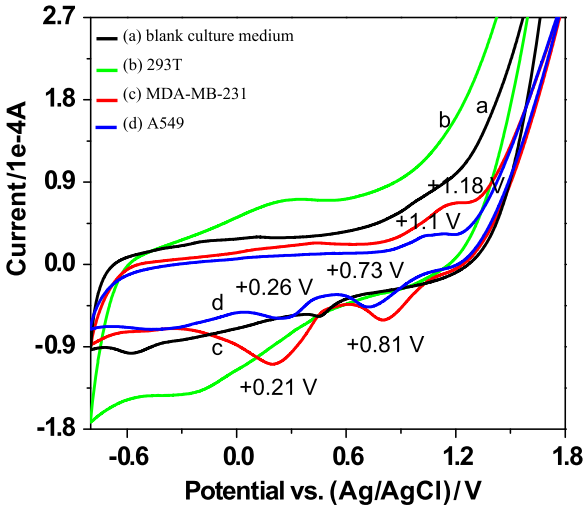

Figure 5. Cyclic voltammograms at the Au/TiO_2 nanobelts modified electrode: (a) blank culture medium, (b) the embryonic kidney cells (293T), (c) the human breast cancer cells (MDA-MB-231) and (d) the human lung cancer cells (A549). Potential sweep rate 100 mV s^{-1}.

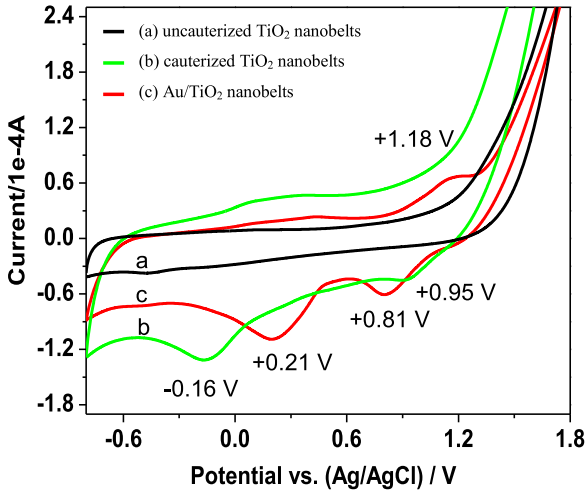

Figure 6. Cyclic voltammograms of human breast cancer cells acquired at (a) uncauterized, (b) cauterized TiO_2 nanobelts and (c) the Au/TiO_2 modified nanobelt electrode. Potential sweep rate 100 mV s^{-1}.

3.2. In situ electrochemical selective determination of cancer cells

In this work, normal embryonic kidney cells (293 T), human breast cancer cells (MDA-MB-231) and human lung cancer cells (A549) were chosen as the illustrating examples, and an Au/TiO_2 modified nanobelt electrode was used as the working electrode. Figure 5 shows the voltammograms of the normal and cancer cells. No redox reaction peaks were observed between −0.8 and +1.8 V with a blank culture medium as the supporting electrolyte (curve a); and similarly, no obvious voltammetric features were for the 293 T normal cells, either (curve b). In contrast, two cathodic peaks at +0.21 and +0.81 V and one anodic peak at +1.18 V can be readily identified for the MDA-MB-231 cancer cells (curve c), whereas two cathodic peaks at +0.26 and +0.73 V and one anodic peak +1.1 V appeared with the A549 cancer cells (curve d). These results show that normal cells (293 T) and cancer cells (MDA-MB-231 or A549) exhibit markedly different voltammetric characteristics, possibly because cancer cells display multiple layers of metabolic alterations that change their microenvironment [24].

3.3. Au/TiO_2 nanobelts with enhanced sensitive determination of cancer cells

Figure 6 compares the performance of pre- and post-modified TiO_2 nanobelt electrodes for sensing breast cancer cells. As shown in curve a in figure 6, no efficient biosensing was observed using a pre-modified TiO_2 nanobelt electrode, probably due to its high electron transfer resistance. Yet after acid etching, the resulting cauterized TiO_2 nanobelts possessed a rough surface and a heterostructure that facilitated adsorption of glycoproteins onto the electrode surface and electron transport through the glycoprotein/cauterized TiO_2 nanobelt electrode interface [25]. In fact, as shown in the electrochemical measurements (curve b), the resulting cauterized TiO_2 modified nanobelt electrode exhibited two cathodic peaks at −0.16 V and +0.95 V, whereas the Au/TiO_2 modified nanobelt electrode showed a new anodic peak at +1.18 V (curve c). In addition, the cathodic peak at +0.81 V in curve c was much sharper than that (+0.95 V) of the cauterized TiO_2 nanobelt electrode (curve b), suggesting that the electron transfer kinetics were markedly enhanced by the incorporation of Au nanoparticles onto the electrode surface layer. Importantly, the additional cathodic peak at +0.21 V in curve c was about 370 mV more positive than that (−0.16 V) of the cauterized TiO_2 nanobelt electrode (curve b), indicating that Au/TiO_2 nanobelts possess electrocatalytic activity with the cathodic peak at −0.16 V. The enhanced biosensing performance might be ascribed to the deposition of Au nanoparticles that facilitated partial electron transfer from titanium to gold as suggested in the XPS measurements (figure 3). Overall the enhanced conductivity and excessive negative charge of the Au nanoparticles resulted in enhanced electron transport and electrocatalytic activity of the TiO_2 nanobelts.

3.4. Enhanced electrochemical sensing mechanism

Multilateral communication between tumour cells, the extracellular matrix (ECM) and neighbouring cells is accomplished through cell adhesion molecules (CAMs), ECM components, proteolytic enzymes and their endogenous inhibitors [26]. CAMs are a kind of glycoproteins on the cell surface. Overexpression or dysregulation of CAMs may cause cancer or tumour metastasis. That is, unlike in a normal cell, some CAMs are often overexpressed in cancer cells. For example, glycoprotein E-selectin and ICAM-1 usually overexpress in various tumour cells, including metastatic breast tumour cells [27], and glycoprotein sialyl-Lewis X possesses high expression in MCF-7 cells [28]. These overexpressed CAMs may be used as tumour markers for cancer diagnosis.

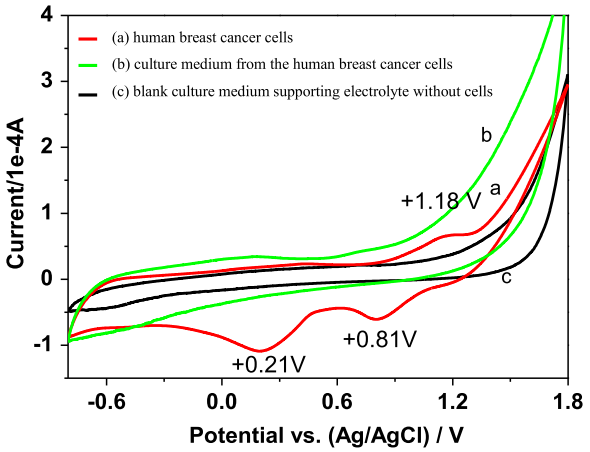

Figure 7. Cyclic voltammograms at the Au/TiO_2 modified nanobelt electrode: (a) the human breast cancer cells, (b) the culture medium from the human breast cancer cells, and (c) blank culture medium. Potential sweep rate 100 mV s^{-1}.

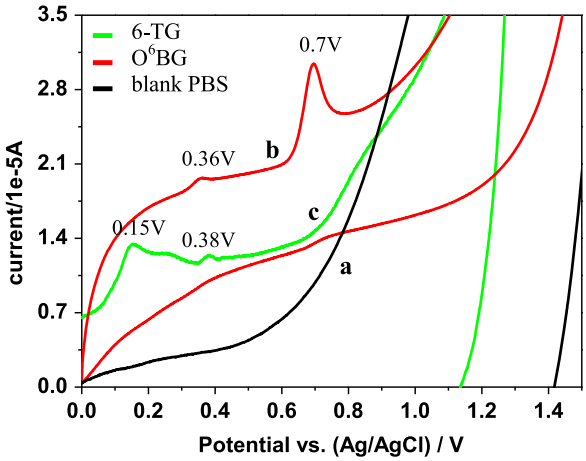

Figure 8. Cyclic voltammograms of an Au/TiO_2 nanobelt electrode in (a) 0.1 M PBS at pH 7.4, (b) 0.1 M PBS at pH 7.4 with 0.1 mM 6-O-benzylguanine (O^6BG), or (c) 0.1 mM 6-Thioguanine (6-TG). Potential sweep rate 100 mV s^{-1}.

A recent study demonstrated that bulky glycoproteins can promote a tumour phenotype in human cells by increasing integrin adhesion and signalling [14].

As described above, the surface and the extracellular matrix of cancer cells overexpress CAMs. When the Au/TiO_2 modified nanobelt electrode is in contact with the breast cancer cells, charge is transferred at the glycoprotein macromolecules/Au-TiO_2 nanobelt interface, resulting in electrochemical reactions. The redox peaks observed above in figures 5 and 6 may be ascribed to the electrochemically redox-active membrane proteins that are overexpressed on the cancer cell surface. The breast cancer cells had different electrochemical signals as their cellular surface microenvironment is different to embryonic kidney cells (293 T). These overexpressed glycoproteins may serve as specific markers for cancer detection by electrochemical technology.

XPS measurements suggest a partial charge transfer from Ti to Au on the TiO_2 nanobelt surface, which led to the accumulation of negative charges on Au nanoparticle surfaces, whereas the n-type TiO_2 was positively charged within the space–charge region. This may facilitate the adsorption of cell surface molecules (i.e. glycoproteins) onto the TiO_2 nanobelt surface and consequently enhance the formation of an electron depletion layer [29, 30]. When the electrode potential was swept negatively, the electrons from the TiO_2 conduction band are driven towards the glycoprotein macromolecule/Au-TiO_2 nanobelt interface to electrocatalytically reduce the glycoproteins. For an n-type semiconductor, the reduction peak current (i) is [31]

$$i = nFAk_f' n_{SC} C_O (x = 0) \quad (1)$$

where n_{SC} (cm^{-3}) is the concentration of electrons at the interface, k_f' ($cm^4\ s^{-1}$) is the heterogeneous rate constant, F is the Faraday constant (96 485 C mol^{-1}), A is the geometrical area of the working electrode ($A = 0.07\ cm^2$), n is the total number of electrons involved in the reduction reaction, and C_O is the reactant concentration. Thus, in comparison with the cauterized TiO_2 nanobelt electrode, the Au-TiO_2 nanobelt electrode exhibited a higher n_{SC} due to gold-doping, which has higher value of i. Additionally, Au nanoparticles at the interface can efficiently improve electron transfer between analyte and electrode surface [32], and hence the interfacial electrocatalytic reduction of glycoproteins. The adsorbed oxygen captured electrons from the conduction band of TiO_2 and formed varied surface active complexes (e.g. superoxo- or peroxo-like species) [33]. These were strong oxidants that facilitated the oxidation of the overexpressed glycoprotein molecules, as manifested in the voltammetric measurements. These unique characteristics are beneficial as they improve the detection sensitivity to cancer cells (figures 5 and 6).

3.5. Specific electrochemical signals from cancer cells

The results described above indicated that cancer cells have different electrochemical characteristics to normal cells. To investigate whether the specific electrochemical signals are derived from cancer cells or from the culture medium, we investigated the electrochemical behaviour of breast cancer cells (MDA-MB-231) by using an Au/TiO_2 modified nanobelt electrode as a working electrode in direct contact with the cells. Two cathodic peaks and one anodic peak were observed at +0.21, +0.81 V and +1.18 V (curve a, figure 7). The culture fluid was then divided into another culture flask, which exhibited no obvious electrochemical signals (curve b). No specific electrochemical signals were observed with a blank culture medium including only a supporting electrolyte either, as depicted in curve c. Soluble glycoproteins are typically present in the intracellular domain, whereas insoluble glycoproteins are present on the surface of cancer cells. Therefore, no electrochemical signal was observed with the divided culture fluid because the interface membrane glycoprotein was insoluble; and the voltammetric responses observed above most likely arose from the surface overexpressed glycoproteins of the breast cancer cells, not from the culture fluid. However, it is currently unclear which redox reactions are responsible for the above voltammetric profiles

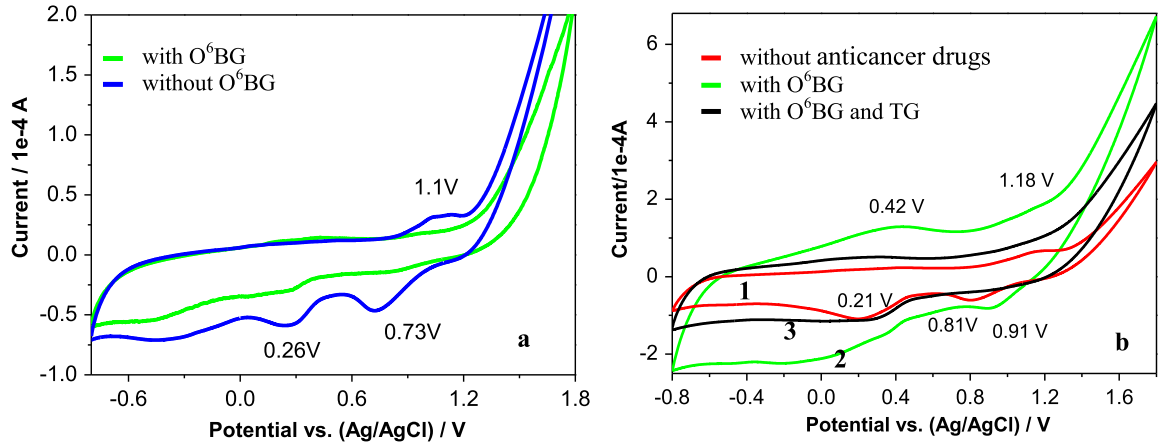

Figure 9. Cyclic voltammograms of an Au/TiO_2 modified nanobelt electrode for lung cancer cells in a culture dish in an RPMI 1640 medium supplemented with 10% fetal calf serum in the absence and presence of 1 μM 6-O-benzylguanine (O^6BG) (a) and for breast cancer cells in a culture dish in DMEM supplemented with 10% fetal calf serum (b) before (1) and after the addition of 1 μM 6-O-benzylguanine (O^6BG) (2) or 1 μM 6-O-benzylguanine (O^6BG) and 1 μM 6-thioguanine (6-TG)(3). Potential sweep rate 100 mV s^{-1}.

for the MDA-MB-231 cancer cells. Further work on the electrochemical reactions of cancer cells will be carried out in the near future.

Clinical studies reveal that large glycoproteins are abundantly expressed on circulating tumour cells from patients with advanced disease [14]. That is, with cancer deterioration, tumour cells passively release their over-expressed CAMs or intracellular soluble glycoproteins into patient's body fluids or blood due to inflammation and cell metastasis or death. In fact, when cancer can be clinically detected, it has already been close to the advanced stage. In contrast, electrochemical detection is a sensitive method that can instantaneously detect a change of even 10^{-19} g of a trace sample and hence realize early cancer diagnosis.

3.6. In situ electrochemical investigation of cancer cells and anticancer drugs effect

O6-benzylguanine (O^6BG) and 6-Thioguanine (6-TG) are important antineoplastic drugs that are commonly used in clinical practice and biochemical research. Figure 8 shows the voltammograms of the Au/TiO_2 nanobelt electrode in 0.1 M PBS (pH 7.4) in the absence and presence of these anticancer drugs. A comparison with the non-oxidizing reaction is shown in curve a for a blank PBS electrolyte. Two irreversible oxidation peaks appear at +0.36 V and +0.70 V for the nanobelt electrodes in the presence of 0.1 mM O^6BG, which can be attributed to the electrooxidation of O^6BG (curve b). In addition, a wide oxidation peak in the potential range of 0–+0.4 V can be attributed to the electrooxidation of 6-TG (curve c).

O^6BG can inhibit DNA replication of tumours due to its irreversible inactivation with O^6-alkylguanine DNA alkyltransferase (AGT). O^6BG, either alone or in combination with other anticancer agents, can also stop the growth of tumour cells [34]. Here, the Au/TiO_2 nanobelt electrode was used to detect the biointeractions between lung cancer cells and the anticancer drug O^6BG. Figure 9(a) shows the cyclic voltammograms of the lung cancer cells at the Au/TiO_2 nanobelt electrode in the absence and presence of 1 μM O^6BG. Two reduction peaks at +0.26 and +0.73 V and one oxidation peak at +1.1 V can be seen in the absence of O^6BG, which may be ascribed to the electrochemical redox of the overexpressed membrane proteins on the cellular surface [19]. When O^6BG was added, the reduction peak at +0.26 V was weakened, and the redox peaks at +0.73 V and +1.1 V actually disappeared. It is clear that the drug caused changes to the cellular membrane, probably due to its rapid bonding with overexpressed membrane proteins [35], causing disruption of the ion channels [36]. These results suggest that Au/TiO_2 nanobelts may serve as promising active materials for exploring and monitoring the relevant biological processes of cancer cells.

Additionally, the Au/TiO_2 nanobelt electrode was employed to detect the biointeractions between breast cancer cells and anticancer drugs. Figure 9(b) shows the cyclic voltammograms of the Au/TiO_2 modified nanobelt electrode for breast cancer cells in the absence and presence of anticancer drugs O^6BG or 6-TG. In comparison with the profiles of breast cancer cells alone (curve 1 in figure 9(b)), after the addition of O^6BG (curve 2) the oxidation peak of the breast cancer cells shifts negatively from +1.18 to +0.42 V, whereas the reduction peak shifts positively from +0.81 V to +0.91 V, implying that an interaction between the surface of the breast cancer cells and O^6BG has occurred. Interestingly, with the further addition of 6-TG, the redox peaks at +0.91 V and +0.42 V disappeared (curve 3). These results indicated that the selective interactions may be different between the cancer cells and O^6BG. O^6BG may not inhibit the DNA replication of breast cancer cells, although it kills lung cancer cells by effective inactivation of AGT (blue curve in figure 9(a)). In addition, O^6BG and 6-TG may have different anticancer efficacy for breast cancer cells. These results suggest that the Au/TiO_2 nanobelts provide a rapid, sensitive and inexpensive method for the detection of anticancer drugs

by *in vitro* screening based on electrochemical sensing technology.

4. Conclusions

Au/TiO_2 nanobelt heterostructures, with Au nanoparticles deposited on the coarsened TiO_2 surface, were successfully prepared and exhibited selective and sensitive detection of cancer cells and biointeractions with anticancer drugs by *in situ* voltammetric measurements. XPS and electrochemical measurements suggested that the Au nanoparticles enhanced the heterostructure conductivity and the electrocatalytic ability of the TiO_2 nanobelts. Electrochemical measurements showed markedly different characteristics for normal cells, cancer cells, and the biointeractions between anticancer drugs and cancer cells, and the electrochemical signals largely arose from the surface proteins of the cancer cells. These results suggest that the electrochemical voltammetry method may serve as a promising technology for specific sensing of tumour cells that will be of significance in early cancer diagnosis, anticancer drug *in vitro* screening and molecular biology research.

Acknowledgments

This research was supported by the National Natural Science Foundation of China (51102152, 61205200), the Cultivation Program of Young Academic Leaders of Zhejiang Province (GK130204217002/001, GK140201202002/001), with startup funds from Hangzhou Dianzi University (KYS195612009), Postdoctoral Science Foundation of China (10000071311003), and Zhejiang Provincial Natural Science Foundation (Grant no. LY12F01005).

References

[1] Liu H Y, Chen D, Li L L, Liu T L, Tan L F, Wu X L and Tang F Q 2011 *Angew. Chem., Int. Ed. Engl.* **50** 891
[2] Fan K L, Cao C Q, Pan Y X, Lu D, Yang D L, Feng J, Song L N, Liang M M and Yan X Y 2012 *Nat. Nanotechnology* **7** 459
[3] Maltzahn G V, Park J H, Lin K Y, Singh N, Schwöppe C, Mesters R, Berdel W E, Ruoslahti E, Sailor M J and Bhatia S N 2011 *Nat. Mater.* **10** 545
[4] Yun Y H, Dong Z Y, Shanov V N and Schulz M J 2007 *Nanotechnology* **18** 465505
[5] Shao N, Wickstrom E and Panchapakesan B 2008 *Nanotechnology* **19** 465101
[6] Zhang H, Sun Y, Wang J, Zhang J, Zhang H Q, Zhou H and Song D Q 2012 *Biosens. Bioelectron.* **34** 137
[7] Cairns R A, Harris I S and Mak T W 2011 *Nat. Rev. Cancer* **11** 85
[8] Kroemer G and Pouyssegur J 2008 *Cancer Cell* **13** 472
[9] Jones P A and Baylin S B 2007 *Cell* **28** 683
[10] Esteller M, Sanchez-Cespedes M, Rosell R, Sidransky D, Baylin S B and Herman J G 1999 *Cancer Res.* **59** 67
[11] Esteller M, Sanchez-Cespedes M, Rosell R, Sidransky D, Baylin S B and Herman J G 2013 *Med. Princ. Pract.* **22** 4
[12] Zhang X A, Lu W J, Shen J Z, Jiang Y X, nHanE, Dong X Y and Huang J L 2015 *Biosens. Bioelectron.* **74** 291
[13] Tse H T K, Gossett D R, moon Y S, Masaeli M, Sohsman M, Ying Y, Mislick K, Adams R P, Rao J and Carlo D D 2013 *Sci. Transl. Med.* **5** 1
[14] Paszek M J *et al* 2014 *Nature* **511** 319
[15] Ilyas A, Asghar W, Allen P B, Duhon H, Ellington A D and Iqbal S M 2012 *Nanotechnology* **23** 275502
[16] Nowicka A, Zabost M E, Donten M, Mazerska Z and Stojek Z 2007 *Anal. Bioanal. Chem.* **389** 1931
[17] Zhang D D, Zhang Y M, Zheng L, Zhan Y Z and He L C 2013 *Biosens. Bioelectron.* **42** 112
[18] Cui J J, Sun D H, Chen S W, Zhou W J, Hu P G, Liu H and Huang Z 2011 *J. Mater. Chem.* **21** 10633
[19] He F, Shen Q, Jiang H, Zhou J, Cheng J, Guo D D, Li Q N, Wang X M, Fu D G and Chen B A 2009 *Talanta* **77** 1009
[20] Feng L Y, Chen Y, Ren J S and Qu X G 2011 *Biomaterials* **32** 2930
[21] Cui J J, Sun D H, Zhou W J, Liu H, Hu P G, Ren N, Qin H M, Huang Z, Lin J J and Ma H Y 2011 *Phys. Chem. Chem. Phys.* **13** 9232
[22] Huang C J, Chiu P H, Wang Y H, Yang C F and Feng S W 2007 *J. Colloid Interface Sci.* **306** 56
[23] Gutiérrez L F, Hamoudi S and Belkacemi K 2012 *Appl. Catal., A* **425-426** 213
[24] Cheong H, Lu C, Lindsten T and Thompson C B 2012 *Nat. Biotechnol.* **30** 1
[25] Soleymani L, Fang Z C, Lam B, Bin X M, Vasilyeva E A, Ross J, Sargent E H and Kelley S O 2011 *ACS Nano* **5** 3360
[26] Bourboulia D and Stetler-Stevenson W G 2010 *Semin. Cancer Biol.* **20** 161
[27] Mastro A M, Gay C V and Welch D R 2003 *Clin. Exp. Metastas.* **20** 275
[28] Jeong H H, Kim Y G, Jang S C, Yi H and Lee C S 2012 *Lab Chip* **12** 3290
[29] Hu P G, Du G J, Zhou W J, Cui J J, Lin J J, Liu H, Liu D, Wang J Y and Chen S W 2010 *ACS Appl. Mater. Interfaces* **2** 3263
[30] Ensafi A A, Taei M, Rahmani H R and Khayamian T 2011 *Electrochim. Acta* **56** 8176
[31] Bard A J and Faulkner L R 2001 *Electrochemical Methods: Fundamentals and Applications* (New York: Wiley) p 752
[32] Zhang S X, Wang N, Niu Y M and Sun C Q 2005 *Sensors Actuators* B **109** 367
[33] Li Q H, Liang Y X, Wan Q and Wang T H 2004 *Appl. Phys. Lett.* **85** 6389
[34] Konduri S D, Ticku J, Bobustuc G C, Sutphin R M, Colon J, Isley B, Bhakat K K, Kalkunte S S and Baker C H 2009 *Clin. Cancer Res.* **15** 6087
[35] Dolan M E, Moschel R C and Pegg A E 1990 *Proc. Natl Acad. Sci. USA* **87** 5368
[36] Cui J J, Ge Y K, Chen S W, Liu H, Huang Z, Jiang H D and Chen J 2013 *J. Mater. Chem.* B **1** 2072